

Microstructural features and mechanical, wear and thermal conductivity characteristics of eggshell derived hydroxyapatite reinforced epoxy bio-composites

Isiaka O. Oladele ¹, Anuoluwapo S. Taiwo ^{1,2*}, Linus N. Onuh ¹, Baraka A. Makinde-Isola ¹

¹ Department of Metallurgical and Materials Engineering, Federal University of Technology, Akure, Ondo State, NIGERIA.

² Enhanced Composites and Structures Centre, School of Aerospace, Transport, and Manufacturing, Cranfield University, Cranfield, UNITED KINGDOM.

*Corresponding author: samuel.taiwo@cranfield.ac.uk

KEYWORDS

Eggshell
Bio-derived
Hydroxyapatite (HAp)
Bio-composites
Mechanical
Wear
Thermal characteristics

ABSTRACT

The research was carried out to stimulate the application of natural materials for the development of bio-composites. The sourced eggshells were processed to obtain eggshell-derived hydroxyapatite particles of 50 μm . Scanning Electron Microscope (SEM) and X-ray Diffraction (XRD) of the eggshell-derived hydroxyapatite particles were carried out while the mechanical, wear and selected physical properties of the developed epoxy-based composites were evaluated. The results revealed that the properties of the bio-derived hydroxyapatite reinforced composites were enhanced compared to the unreinforced epoxy matrix. For most of the tests carried out, optimum results were obtained at different weight fractions. However, 15 wt.% eggshell-derived hydroxyapatite reinforced epoxy composite emerged as the weight fraction with the highest optimum values. The sample possessed a value of 0.098 for wear index, 42.947 MPa for maximum flexural strength, 37.67 HS for hardness, 0.4413 W/mK for thermal conductivity, and 41.3 J for impact properties. Structural viability of the developed bio-composites as biomedical materials was discovered as well as the suitability of non-synthetic HAp as a replacement for synthetic HAPs.

Received 20 November 2021; received in revised form 20 January 2022; accepted 18 February 2022.

To cite this article: Oladele et al. (2022). Microstructural features and mechanical, wear and thermal conductivity characteristics of eggshell derived hydroxyapatite reinforced epoxy bio-composites. *Jurnal Tribologi* 35, pp.68-91.

1.0 INTRODUCTION

Due to the accelerating development of new technologies, it is safe to say that composite materials have been integrated into all sectors of human activity (Oladele et al., 2020a). The emergence of this special class of material is due to human curiosity and ingenuity, which was majorly based on economic considerations and mechanical performance. To this end, research has gained momentum, in the last few years, natural biological wastes have found numerous applications in ecology and biomaterials (Oladele et al., 2021; Araya et al., 2019). Composites have a unique characteristic in the sense that they display a blend of the best characteristics of each material (Oladele et al., 2019; Bello et al., 2015). The distinctive features of composite material are strongly hinged on the type and shape of reinforcement embedded in the matrix.

The most effective and readily accessible form of composite presently in use today is the polymer-based composite because they possess high cost and performance efficiency owing to their simple fabrication methods and low production cost (Thomas et al., 2012). The use of unreinforced polymers for structural applications is currently watered-down due to their poor mechanical properties such as low strength, low modulus, and low impact resistance. Reinforcement of polymers with natural bio-derived and bio-degradable particles enhances the manufacture of polymer-based composites, that is characterized by possessing good abrasion resistance, good fatigue resistance, high fracture resistance, high specific stiffness, good corrosion resistance, high specific strength, good impact resistance, and most importantly, cost-effectiveness (Shuhadah et al., 2008).

The eggshell gotten from the chicken eggs is a bioceramic material in which the mineral calcium carbonate in the form of polymorphous calcite is closely linked with the organic matrix (Nys et al., 2004). The inorganic component of the chicken eggshell comprises columnar crystal layers and spherulitic attached to the shell casings. The size and prearrangement of crystals vary diagonally across these layers (Ahmed et al., 2005). Eggshells are used in composite materials as the source of calcium filler owing to the presence of calcium carbonate (Oliveira et al., 2016) and previous research has revealed that they have a significant influence on various products that requires calcium filler (Oladele et al., 2020a). Although, several attempts have been made to use the components of eggshell obtained from chicken eggs for various applications, the availability of this eggshell and its inherent composition chemically, makes it a viable source of filler material in developing polymer-based composites (Shuhadah et al., 2008). Research has revealed that eggshells from chicken eggs possess a comparatively low density when compared to the inorganic calcium carbonate which enhances mechanical properties when used as reinforcements in polymer composites (Patricio et al., 2007).

Hydroxyapatite is a ceramic-based material containing calcium phosphate which was discovered to be highly essential and paramount as a biomaterial by virtue of its osteophilic character and its integration into bone tissues (Duchyene et al., 1986; Agbabiaka et al., 2020). Natural human bones comprise inorganic and organic composite primarily consisting of collagen fibers and nanostructured hydroxyapatite ($\text{Ca}_{10}(\text{PO}_4)_6(\text{OH})_2$) (Mulijani and Sulisty., 2012). Hydroxyapatite has been discovered to be the main component responsible for the development of the mineral segment of teeth and bone tissue, and it is a major prerequisite in the field of biomaterials when considering the growth and development of bone implants (Elizondo-Villarreal et al., 2012). Hydroxyapatite has several areas of importance in tissue engineering, owing to its outstanding biocompatible and bioactive nature having a comparable biological and chemical composition with the inorganic part of the human bone (Oladele et al., 2018a).

Alizadeh-Osgouei et al., (2018) in a comprehensive review stated that biomaterials as a necessity must showcase a combination of apposite properties to be recommended for a particular area of applications, such properties may include durability, strength, and biodegradability influence. In the same way, certain metallic materials and their corresponding alloys such as cobalt, stainless steel, titanium, and its alloys were extensively explored as materials for an implant and for several biomedical equipment applications for the reason of their outstanding mechanical properties. Nonetheless, these exceptional materials may sometimes develop biological problems like poor tissue adhesion, stress shielding, and toxicity effect because of their modulus of elasticity that is relatively high. To alleviate many of these problems, hydroxyapatite reinforced composites or their respective coatings may be used on these metallic materials since their chemical composition is highly similar to that of human bones and teeth.

The dire need for improved biomedical materials cannot be overemphasized and this has led many researchers to begin an investigation into the development of new biomaterials that are sourced from environmentally friendly and sustainable agricultural products (Agbeboh et al., 2020) which could serve as alternative reinforcing fillers, in developing polymer-based biomaterials to solve biomedical related problems. The purpose of this work was to develop sustainable bio-composites from agro-based by-product (chicken eggshell) that is usually regarded as waste in many countries of the world like Nigeria where they are readily available. In this research, waste chicken eggshells were procured and processed to obtain bio-derived HAP that was used for the development of epoxy-based bio-composites targeted for biomedical applications.

2.0 MATERIALS AND METHODS

2.1 Materials

The materials used for the research include the following: Epoxy Resin and Hardener (for epoxy resin) which were supplied from Malachy Enterprise, Lagos. Eggshells were obtained from the eggs of 20-week-old brown chicken (*Gallus domesticus*), of frizzled feather and fluffed neck structure with an average body weight of 0.7 ± 0.24 kg. Distilled water and Orthophosphoric acid were purchased at Pascal Scientific Ltd., Akure Ondo State, Nigeria.

2.2 Preparation of Egg Shell Based Hydroxyapatite Particle

The preparation of the eggshells to hydroxyapatite particles required a series of steps following the procedure carried out by Agbabiaka *et al.* (2020). The calcination process was done using an oven with model number KX350A; KEN XIN International Company Limited, China) at 80 °C to remove moisture from the eggshell. Figure 1 shows the image of eggs and eggshells.

The calcination process begins by heating the eggshells from room temperature to 550°C at a heating rate of 7°C /min and holding at this temperature for 2 hours, followed by subsequent heating to a temperature of 700°C at a rate of 5°C /min and another holding time of 2 hours. The final stage of the calcination process involved a lower heating rate of 4°C /min to a maximum temperature of 1000°C and a further holding time of 1 hour at this temperature. At this point, the eggshells have completely transformed to calcium oxide (CaO) by giving off carbon dioxide (CO₂). The CO₂ was formed through Equation (1)

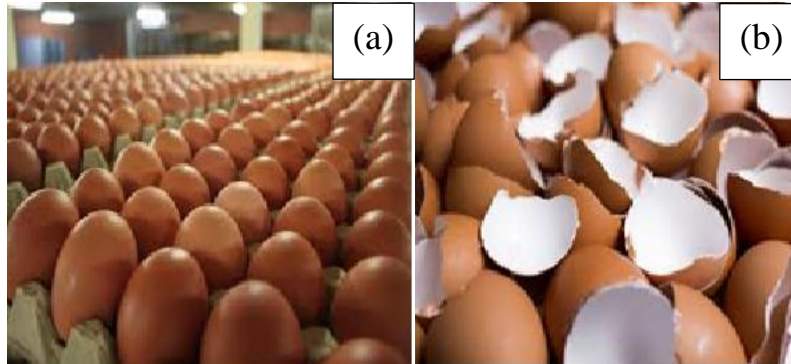


Figure 1: (a) chicken eggs (b) chicken eggshell.



The synthesized eggshell-derived hydroxyapatite is as shown in Figure 2.



Figure 2: Synthesized eggshell derived hydroxyapatite.

2.3 Fabrication of Eggshell Derived Hydroxyapatite Composites

The eggshell-derived hydroxyapatite reinforced epoxy composite specimens were produced via the stir cast molding process. The bio-derived epoxy-based composites were formed by dispersing 3, 6, 9, 12, and 15 wt.% hydroxyapatite particles (HAp) randomly in epoxy resin (in ratio 2:1 with its hardener). A total of 350 g was also used to calculate the mass of the matrix and reinforcement in the production of the composites with the formulation shown in Table 1. Unreinforced epoxy-based specimen denoted as the control specimen was first developed to stand as the basis of comparison and for the fabrication of the composites. Samples of the developed composites are as shown in Figure 3 comprising wear, tensile, flexural, and impact test samples from left to right, respectively.

Table 1: Volumetric ratio of the developed epoxy bio-composite.

Weight (%)	Epoxy Resin (g)	Hardener (g)	Egg Shell HAp (g)
3	226.33	113.16	10.50
6	219.33	109.66	21.00
9	212.33	106.17	31.50
12	205.33	102.67	42.00
15	198.33	99.17	52.50

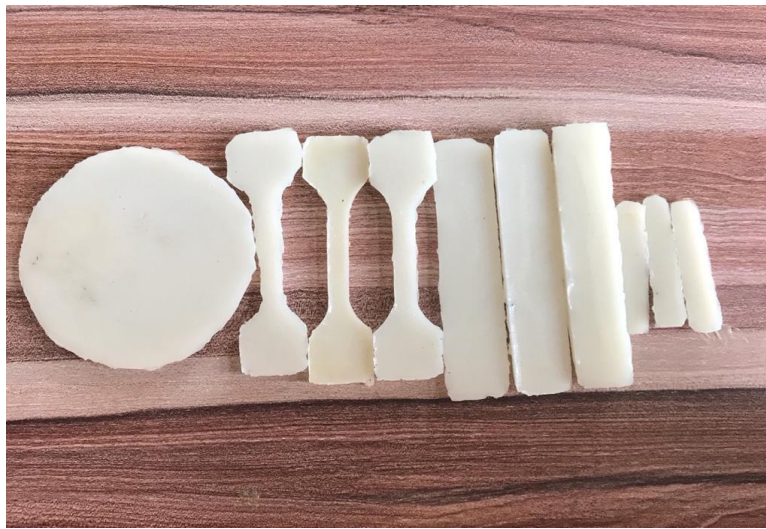


Figure 3: Fabricated eggshell derived hydroxyapatite-based epoxy bio-composite samples for wear and mechanical properties tests.

The fabricated eggshell derived hydroxyapatite-based epoxy bio-composite samples have the following scale: Wear sample- 100 mm diameter and 3 mm thickness; Tensile samples- 115 mm length and 3 mm thickness; Flexural samples- 150 mm length, 50 mm width, and 3 mm thickness; Impact samples- 64 mm length, 11 mm width and 3 mm thickness

2.4 Characterization and Evaluation of Eggshell and Developed Bio-Composites

X-Ray diffraction (XRD) pattern of the eggshell particles was carried out to determine the phases present in the particles by taking measurements within the range of $2\theta = 10 - 90^\circ$ using a Shimadzu XDS 2400H diffractometer with 40 mA, 45 VA, and 240 mm with a copper $K\alpha$ radiation source. The machine was operated over generator settings of 30 kV and 20 mA at a temperature of 25°C and the patterns were analyzed using PANalytical (v3.0e) X'pert High score software.

2.4.1 Tensile Test

Tensile testing on the samples was performed on a universal testing machine (UTM) with a model number FS 300–1023, USA using a crosshead speed of 5 mm/min. ASTM D-638-14 standard was followed while carrying out the test at an ambient temperature of $24 \pm 2^\circ\text{C}$. Samples dimensions were achieved following Type IV description having a total length and thickness of 115 mm and 3 mm, respectively.

2.4.2 Flexural Test

Following ASTM D-790-15 standard, a flexural test was conducted on the composite's samples with the aid of a universal testing machine. Three samples were tested from each set of composites developed following the standard. The dimension of the test specimen was measured to be 150 × 50 × 3 mm while the test was performed at a crosshead speed of 5 mm/min.

2.4.3 Hardness Test

A digital Shore Hardness Tester was used to perform the hardness test. The measurement and determination of the hardness of each material were achieved using the hardness testing machine which expresses its values in terms of HRC. For every sample tested, six random indentations were made on the sample while each indentation was affected at different locations on the sample. Using a load of 15 kg, each sample was tested over a 15 second dwell time. An average value was calculated to obtain the mean value hardness which was used for plotting the result for each selected sample.

2.4.4 Impact Test

Impact test on the samples was conducted under ASTM D256-10 (2018) standard using notched samples. The test was carried out using a Hounsfield balanced impact testing machine with serial number 3915 and model h10-3. The dimension of the impact test samples measuring 64 × 11 × 3 mm were notched at the middle. Samples were horizontally positioned on the testing machine while keeping a gap of 60 mm from each line of supports. Samples were placed on a cantilever and clamped in a vertical position with a V-notch at the top level of the clamp. The pendulum of the machine is allowed to strike the test piece as it falls freely from a predetermined height.

2.4.5 Wear Test

The wear resistance of the samples was examined using a Taber abrasion machine (Model 5135, USA) following ASTM D4060-10 standard. Fixing the test piece to the Taber abrasion tester requires drilling a center hole of 10 mm on the test samples. The samples were secured firmly to the testing platform of the machine which is controlled by a driven motor at 500 rpm. Each sample was in the form of a flat round disc measuring about 100 mm in diameter with a standard thickness of approximately 3 mm. The wear resistance of the samples was calculated as a function of weight loss at a predetermined number of abrasion cycles (500) following ASTM D4060-10 standard. A set of two clockwise rotating abrasive wheels measuring 50 mm diameter and 12.6 mm thickness rob against the test samples with a contact load of 1000 g, using a 500 rpm rotational speed for about 1000 cycles. Equation (2) presented the calculation for the wear indices of the samples based on the sample weight loss.

$$\text{Wear Index} = \frac{(W_i - W_f)}{c} \times 1000 \quad (2)$$

Where, W_i , W_f and C are initial weight, final weight, and the number of test cycles, respectively.

2.4.6 Thermal Conductivity Test

Lee's disk apparatus was used to determine the thermal conductivity of the developed composite samples following ASTM E1530-19 (2019). A temperature range of 50°C – 80°C was considered sufficient for the thermal conductivity analysis of the samples in order to avoid the introduction of thermal degradation of samples at a higher temperature which may be closer to the initiation of thermal degradation in the developed composite samples (Thomas *et al.*, 2012). Equation (3) was employed to calculate the thermal conductivity of the composite samples.

$$K = \frac{m cp(\Phi_1 - \Phi_2)4x}{\pi D^2(T_1 - T_2)t} \quad (3)$$

Where, K is the thermal conductivity, m is the mass of the disk (0.0078 kg), Cp is the specific heat capacity of the disk (0.91 kJ/kg K), Φ_1 and Φ_2 are the initial and final temperatures of the disk B, D is the diameter of the sample (0.04m), x is the thickness of the sample (0.003 m), T_1 and T_2 are the temperatures of disk A and B in Kelvin and, t is the final time taken to reach a stable temperature.

2.4.7 Water Absorption Test

To perform the water absorption test on the composite samples ASTM D5229M-12 (2012) was followed. A 500 ml of clean water was poured into a 1 L plastic basin. Before submerging the samples in water, the initial weight of each sample was taken using an electronic weighing balance, and subsequent readings were taken every day for the next 30 days. Before taking any readings, the samples were brought out from the water, damped with a dry clean cloth, and then placed on the weighing balance while recording the values displayed on the screen. The data collected were used to calculate the weight gained by each sample using the formula in Equation (4).

$$W(g) = W_t - W_o \quad (4)$$

where W (g) is the weight gained per day, W_o is the initial weight or dry weight of the sample before submerging in water and, W_t is the weight of the sample after soaking in water for the time (t).

2.4.8 Microscopy Characterization

The SEM images characterization for the fracture surfaces of the samples was performed using EVO MA 15, Carl Zeiss SMT. Each fractured Sample was first gold-sputtered with a thin layer of gold to improve electrical conductivity.

3.0 RESULTS AND DISCUSSION

3.1 Tensile Properties

Figure 4 showed the effects of the addition of eggshell-derived HAP reinforcements on the maximum tensile strength of the fabricated composites. It was observed that there were enhancements in the maximum tensile strength from the addition of eggshell-derived HAP reinforcement particles when compared to the unreinforced epoxy. The 3 wt.% reinforced composite possessed the optimum result for maximum tensile strength with a value of 31.27 MPa showing a 40.34 % enhancement when compared to the unreinforced epoxy with a value of 22.45 MPa. This enhancement might have occurred due to the presence of CaCO_3 in the HAP. Oladele *et*

al. (2019) in their study on the structural performance of poultry eggshell-derived hydroxyapatite-based high-density polyethylene bio-composites revealed that enhancement in tensile strength was highly supported by the presence of particulate CaCO_3 in the developed hybrid composites which agreed with the findings of this work. Bhaskar and Singh (2013) in their study on physical and mechanical properties of coconut shell particle reinforced-epoxy composite also confirmed that the increase in density (weight fraction) of epoxy composites decreases the tensile strength.

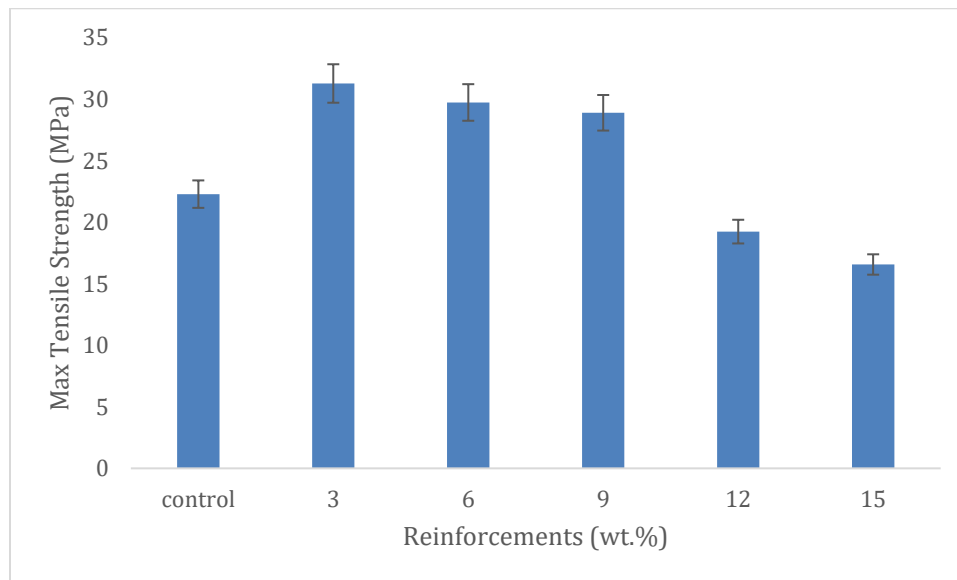


Figure 4: Effects of eggshell derived HAp on maximum tensile strength.

Figure 5 shows the effects of eggshell-derived HAp on the tensile strain at maximum tensile strength. The unreinforced epoxy possessed the longest tensile strain at maximum tensile strength. Thus, the longest elongation per unit length at its peak stress with a strain value of 0.038 mm/mm. The unreinforced epoxy when compared to the reinforced composites has a relatively high strain rate. The 3 wt.% reinforced composite has a better strain rate when compared to other reinforced composites with a value of 0.02784 mm/mm also indicating a 35.55 % decrease from the unreinforced epoxy. There was an occurrence of a steady decrease in the tensile strain rate as the weight fraction increased. This occurrence was due to the increase in the stiffness and strength caused by the increase in the weight fraction of the eggshell derived HAp in the epoxy matrix which was part of the reasons for improved impact energy obtained in the samples. It is safe to say that the reinforced composites would not be suitable for load-bearing applications since they possess lower strain rate values when compared to the unreinforced epoxy.

Figure 6 shows the effects of eggshell-derived HAp on tensile modulus. It was observed that enhancements occurred due to the presence of the eggshell-derived HAp. The 9 wt.% reinforced HAp bio-composite possessed the optimum tensile modulus enhancement when compared to other weight fractions with an optimum value of 2112.566 MPa thereby indicating a 368 % increase when compared to the unreinforced epoxy and a 226 % increase when compared to the 15 wt.% composite (which shows the lowest enhancement with a value of 674.9 MPa). The

maximum tensile strength and tensile strain values as shown in Figure 1 to Figure 3 are important integrals in determining the tensile modulus properties since the tensile modulus indicates the ratio of the tensile stress to the true strain (Kolawole *et al.*, 2019). The low enhancements in the reinforced composites may have occurred due to the presence of agglomeration in the matrix due to higher weight concentration or the insufficient wetting of the filler at higher weight concentration.

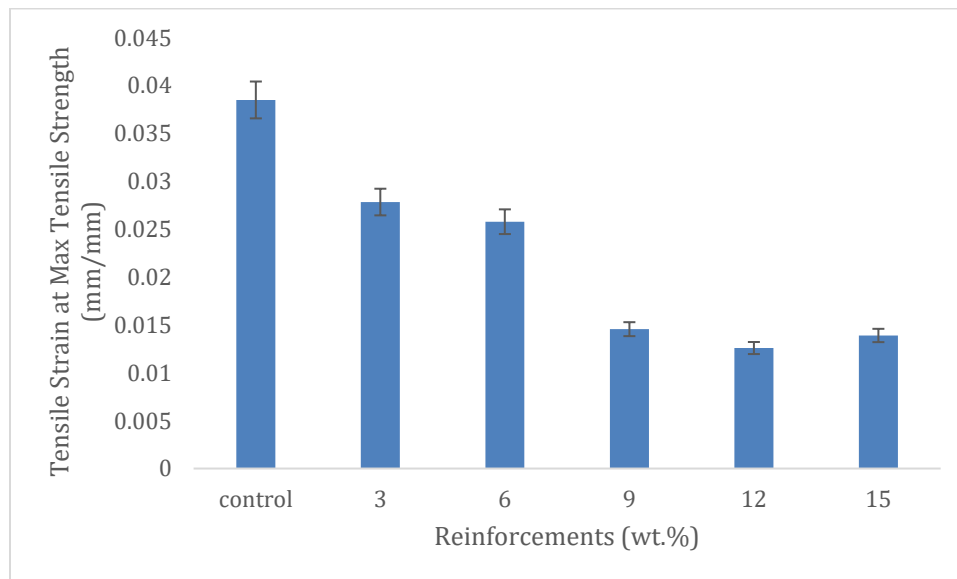


Figure 5: Effects of eggshell derived HAP on the tensile strain at maximum tensile strength.

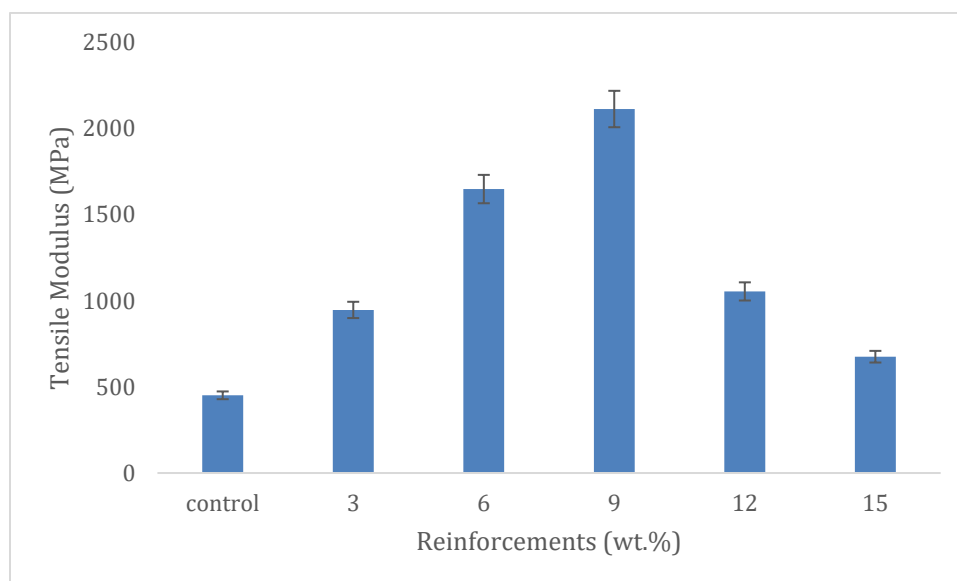


Figure 6: Effects of eggshell derived HAP on the tensile modulus.

3.2 Flexural Properties

Figure 7 presents the variation of eggshell-derived HAp reinforcements on maximum flexural strength. It was detected that there were no visible enhancements in the maximum flexural strength from the addition of eggshell-derived HAp. Reinforcement particles developed from animal wastes have been discovered to enhance the mechanical properties of polymer composites (Oladele *et al.*, 2016). The 15 wt.% HAp reinforced bio-composite possessed the optimum visible result for maximum flexural strength with a value of 42.94 MPa indicating a 3.74 % improvement compared to the unreinforced epoxy which has a value of 41.39 MPa. It was observed that the maximum flexural strength increased with a simultaneous increase in the weight fraction of HAp reinforcement. This enhancement in the maximum flexural strength of the 15 wt.% bio-composite may have occurred due to the presence of CaCO₃ in the eggshell-derived HAp. This CaCO₃ present in the HAp contains hydroxyl, amine, and carboxyl groups which enhance the covalent bonding of oxygen (present in the HAp) and hydrogen (present in the epoxy resin) (Owuamanam, 2019).

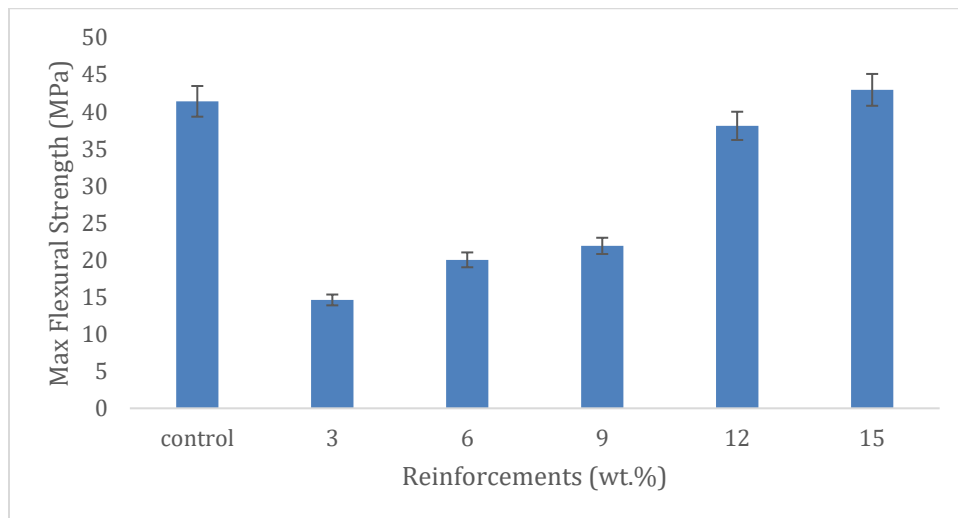


Figure 7: Effects of eggshell derived HAp on maximum flexural strength.

Figure 8 shows the effects of eggshell-derived HAp on flexural strain at maximum flexural strength of the developed composites. There was no enhancement of any kind on the reinforced composites when compared to the unreinforced epoxy and this indicates that the reinforced composites possess a lower flexural strain rate when compared to the unreinforced epoxy. This poor enhancement in the flexural strain may have occurred due to the presence of agglomeration in the matrix.

Figure 9 shows the variation of the eggshell-derived HAp weight fractions on flexural modulus. It was observed that no enhancement occurred in the flexural modulus property of the developed bio-composite when compared to the unreinforced epoxy. However, a steady drop in the flexural modulus of the composite was noticed to be consistent with an increase in the reinforcement contents from 3 – 12 wt.%, followed by a sudden drop at 15 wt.% HAp contents. This poor behaviour in the flexural properties of the composites may have occurred due to the simultaneous flexural stress/strain ratio. Furthermore, poor adhesion at the particle-matrix interface between

the eggshell-derived HAp particles and the epoxy matrix may have also resulted in the weak flexural modulus properties observed in the developed bio-composites.

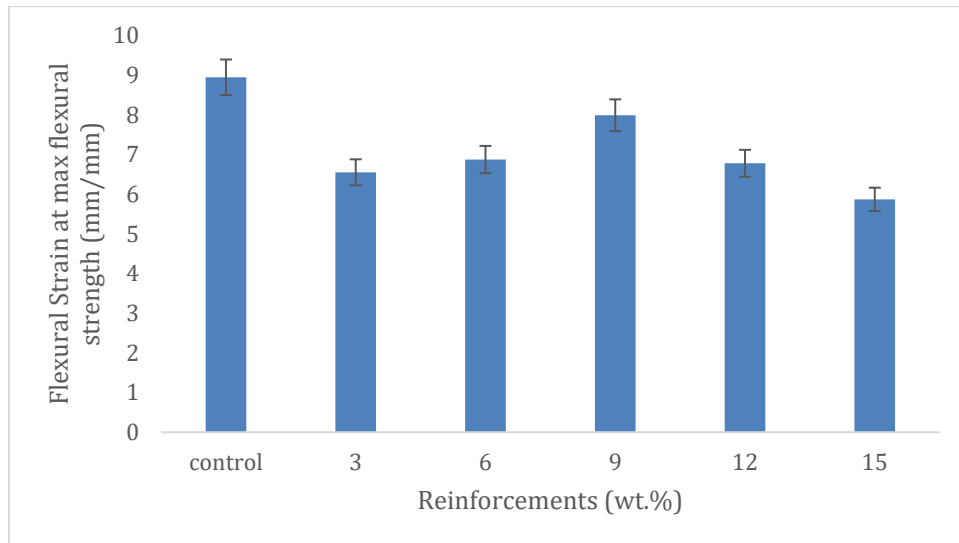


Figure 8: Effects of eggshell derived HAp on flexural strain at maximum flexural strength.

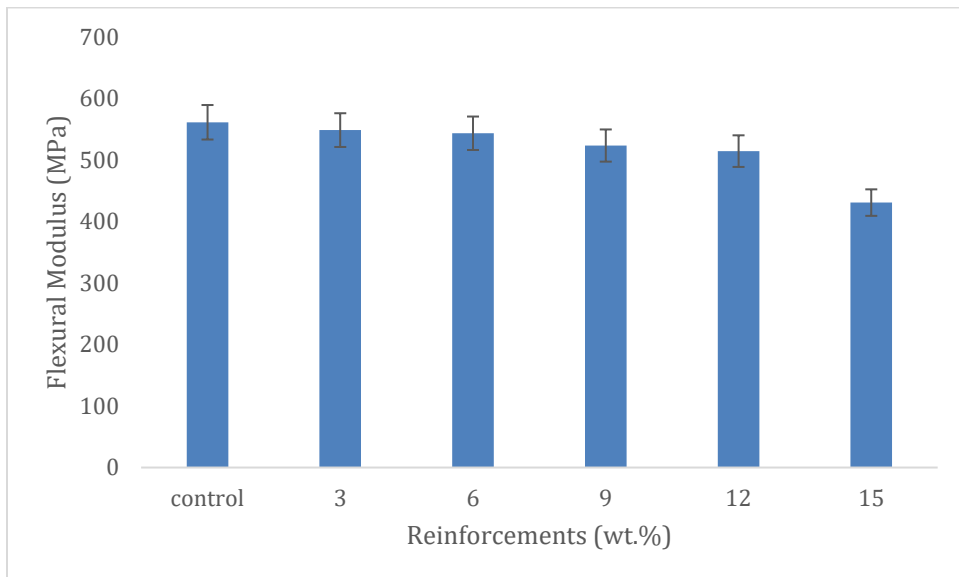


Figure 9: Effects of eggshell derived HAp on Flexural Modulus

3.3 Hardness Properties

Figure 10 presents the hardness properties of the unreinforced and reinforced bio-composite samples. The result indicated that the hardness was lowest in the unreinforced epoxy and gained

a peak hardness value in the 15 wt.% HAp reinforced epoxy composite with a value of 37.67 HS. The hardness property increased concurrently as the reinforcement contents increases from 3 wt.% to 15 wt.% respectively, indicating a 12.03 % improvement in the hardness property of the reinforced composites of 3 wt.% and 15 wt.%. This resulted in a 231.6 % enhancement in the 15 wt.% HAp bio-composite when compared to the unreinforced epoxy (with a value of 11.36 HS) which had the least hardness value. These increase in the hardness properties occurred due to the simultaneous increase in the weight density of the composite as the weight fraction increases (Oladele *et al.*, 2018b). It could also have occurred due to the proper filling of the HAp reinforcement in the epoxy matrix, leading to the absence of pores in the developed bio-composites as the weight fraction increases.

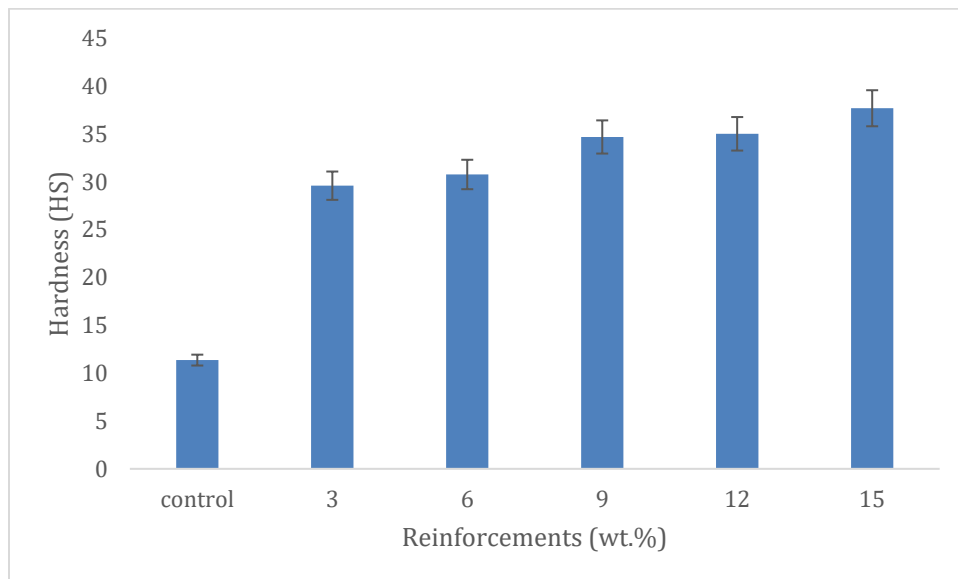


Figure 10: Effects of eggshell derived HAp on the hardness property.

3.4 Impact Properties

The variation of impact energy on the addition of reinforcement is shown in Figure 11. The result detects a simultaneous increase in the impact energy as the reinforcements increase. The unreinforced epoxy absorbed the lowest amount of impact energy before fracture with an exact value of 25.5 J while the 15 wt.% reinforced sample possessed the best possible impact energy with a value of 41.3 J showing a 61.96 % increase from the unreinforced epoxy. Oladele and Isola (2016) in their study concluded that the increase in weight fraction yields a simultaneous increase in the weight density. This weight density improves the strength and fracture toughness of the composites. Also, Teboho *et al.*, (2018) in their study confirmed that the increase in the weight fraction of reinforcements improves the impact energy of the composites.

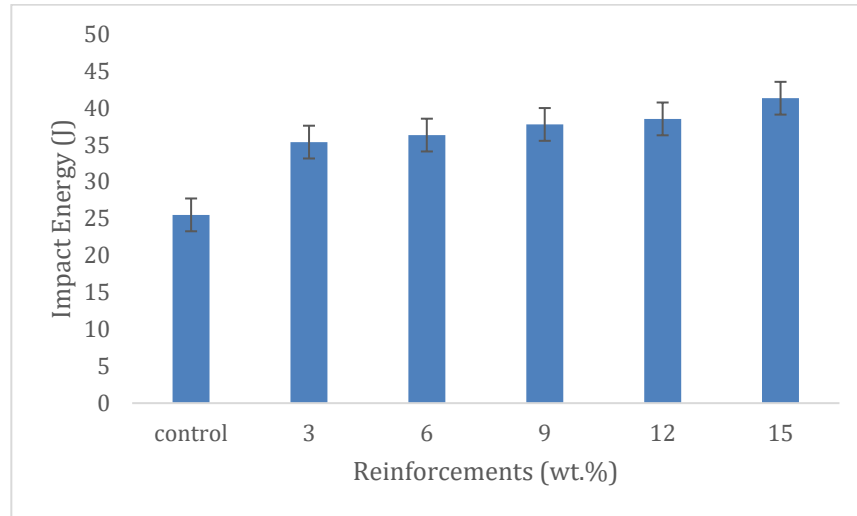


Figure 11: Effects of eggshell derived HAp on impact energy.

3.5 Thermal Conductivity Properties

Figure 12 shows the effect of eggshell derived HAp reinforcements on thermal conductivity. The thermal conductivity of the unreinforced epoxy had the lowest when compared to other reinforced samples with a value of 0.1134 W/mK. It also shows a simultaneous increase with increasing weight percent revealing a 290% increase from the unreinforced epoxy to the 15 wt.% reinforced composite. Oladele *et al.*, (2020b) in their work stated that low thermal conductivity yields higher resistance to temperature changes. The 15 wt.% reinforced sample possesses the highest thermal conductivity with a value of 0.4413 W/mK. In general, the thermal conductivity of the eggshell was progressively higher for eggshell reinforced samples when compared to the eggshell reinforced samples. From the results observed in Figure 12, it was evident that the inclusion of eggshell bio-derived HAp improved the thermal conductivity properties of epoxy, and this supports the conclusion that this material can be utilized as thermal conductive material if properly modified with specified weight fractions. Other farm animal waste-based materials could be processed as alternative sources to the synthetic materials currently used, thus, promote the development of biodegradable and sustainable materials for biomedical applications.

3.6 Water Absorption Properties

The variation of water absorption properties on control and eggshell-derived HAp reinforced samples is shown in Figure 13. This reveals the behavior of the samples when immersed in water medium against time. It can be observed from Figure 11 that as the reinforcement weight fraction increases, the weight gained (water intake) by the composite samples increases from control to the 15 wt.% simultaneously. This increase in weight occurred due to the increased weight fraction of the eggshell-derived HAp. The eggshell-derived HAp particles in the epoxy enhance the rate of water absorption in the epoxy composites by retaining water which aids in transmitting oxygen and ions in the epoxy matrix. It can also be seen that all the samples absorbed water rapidly and linearly at the initial stage before the saturation level was attained from day 27 where further increase in water absorption was not noticeable till day 30. Oladele *et al.*, (2020b) in their research on the Thermal Stability, Moisture Uptake Potentials and Mechanical Properties of Modified Plant-

Based Cellulosic Fiber-Animal Wastes Hybrid Reinforced Epoxy Composites stated that according to Fick's law which measures the amount of substance that will flow through a unit area during a unit time interval, diffusion of water in the polymer will also obey the law. Water aids in transmitting oxygen and ions, hence, diffusion of water in polymers is an important mechanism that involves intensive attention. From Figure 11, the rate of water absorption from day 0 to day 15 was rapid which shows a steep slope on the curve while from day 16 till day 24, there was a linear and gradual rate of water absorption which indicated a near saturation of the samples. From day 25 till day 31, it was observed that the samples were saturated all through. There was a flat and saturated mode in the curve. In general, the 15 wt.% reinforced sample possessed the highest weight gain amongst all.

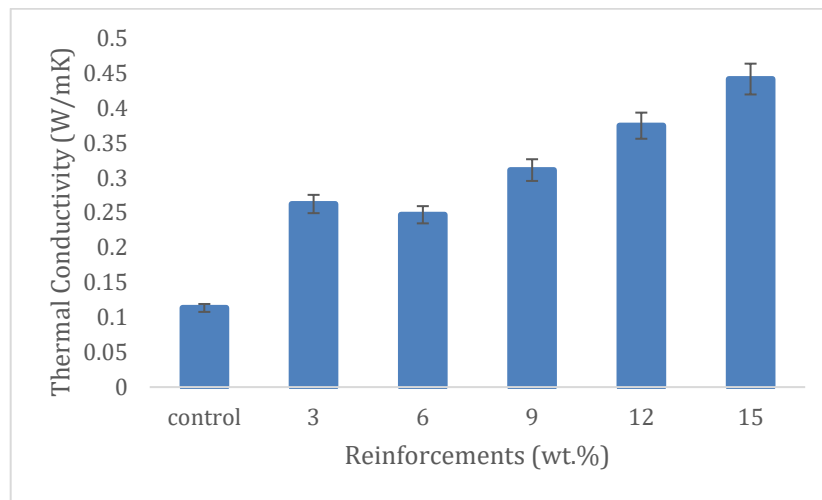


Figure 12: Effects of eggshell derived HAp on thermal conductivity of epoxy composites.

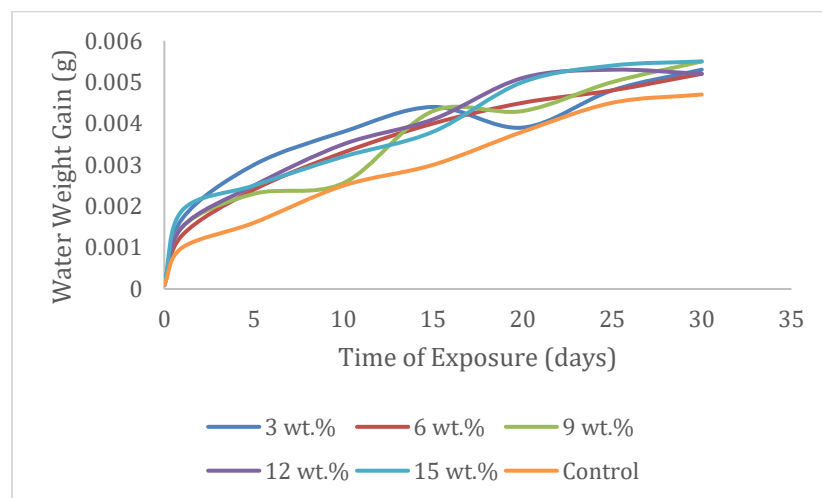


Figure 13: Variation of water absorption properties with the composites.

3.7 Wear Properties

Figure 14 revealed the wear index of the samples. It was observed that the unreinforced epoxy possesses the highest wear index (0.342) when compared to the reinforced samples which depict low wear resistance. Hence, there was a 71.34% enhancement in the wear index from 15 wt.% reinforced composite when compared to the unreinforced epoxy. Therefore, the presence of eggshell-derived HAp in epoxy composites improves wear resistance when compared to samples without reinforcement.

The resulting low frictional force existing from the increase in weight fraction agreed with Balan *et al.*, (2020) in their study on the investigation on water absorption and wear characteristics of waste plastics and seashell powder reinforced polymer composite concluded that wear resistance increases with an increase in weight fraction. Daramola *et al.*, (2020) concluded in their study that an increase in reinforcements improves wear resistance and at the same time improves shear strength. Also, the low frictional force had been proved to occur in reinforced epoxy composites due to the presence of reinforcements that possess high density than the epoxy matrix (Ramesh *et al.*, 2014). From the results, it was observed that the control sample possessed the highest wear index, and the value reduces gradually till the 15 wt.% HAp additions indicating a 71.34 % decrease. Thus, the 15 wt.% HAp reinforced epoxy bio-composites possessed the highest wear resistance with an optimum value of 0.098. The reduction in wear index indicates an increase in wear resistance properties.

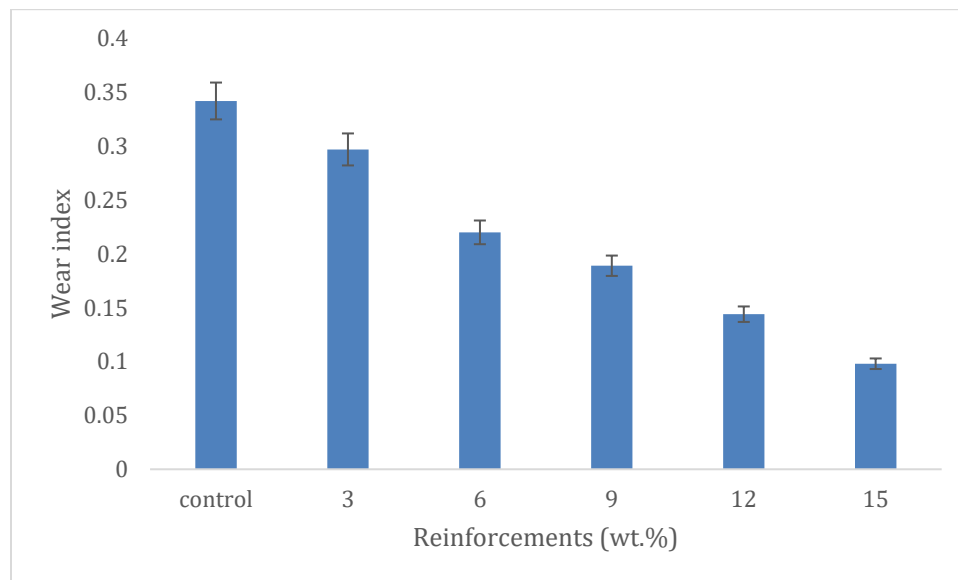


Figure 14: Effects of eggshell derived HAp on wear index of epoxy-based composites.

3.8 XRD analysis and SEM Image of Eggshell Derived HAp Particles

The XRD analysis of the eggshell powder was carried out using a Shimadzu XDS 2400H diffractometer with 40 mA, 45 VA, and 240 mm tube current, voltage rating, and goniometer radius, respectively, attached to the digitized computer along with graphical assembly on uncompressed powders to collect the maximum of the diffraction lines and better identification of the phases. The powdered sample was prepared using the sample preparation block,

compressed into the sample pouch to create a smooth surface. The sample was then placed on the sample stage in the XRD cupboard. The X-ray of Cu K α radiations was collimated and directed onto the sample. Then, the powdered sample was analyzed using the reflection-transmission spinner stage and Theta-Theta settings scanning range of 4 to 75.000 degrees with a two-theta step of 0.026 at 13.7700 seconds per step. The intensity of the diffracted X-rays is continuously recorded automatically on a chart and the appropriate θ and (d) values were then obtained as the sample and detector were rotated through their respective angles.

Fixed anti-scatter and divergence slits of $\frac{1}{4}^\circ$ were used together with a beam mask of 10 mm. All scans were carried out in continuous mode using a detector. The d (111) spacing (\AA) was determined using Bragg's law shown in equation (5).

$$\text{\AA} = \frac{\lambda}{2 \sin(2\theta/2)} \tag{5}$$

Where λ is the K α wavelength and 2θ is the peak value at the $2\theta^\circ$ axis.

The diffractogram for the samples was obtained. The obtained experimental patterns were compared to standards compiled by Joint Committee on Powder Diffraction and Standards (JCDPS), while the 2-theta angles, d-spacing, and relative intensities were shown in Table 2 below.

Table 2: XRD diffraction peaks of eggshell derived HAp particles.

Peak	2 θ /degree	Plane	Intensity	d-Value (\AA)	Mineral Phase
1	12.18	110	49.30	7.7260	Calcium carbonate
2	14.24	001	49.64	6.2146	Apatite
3	19.04	101	86.11	4.6572	Hydroxyapatite
4	20.13	020	81.84	4.4080	Kuesiterite
5	21.47	111	91.37	4.1358	Dolomite
6	22.64	120	110.25	3.9241	Hydroxyapatite
7	29.97	211	486.31	2.9793	Hydroxyapatite
8	30.52	121	126.38	2.9267	Otavite
9	32.70	220	80.06	2.7709	Calcite
10	43.18	130	92.50	2.0935	Ovocalyxin-32
11	43.82	221	130.47	2.0643	Hydroxyapatite
12	44.75	002	81.84	2.0236	Quartz
13	45.76	261	52.83	1.9812	Hydroxyapatite
14	51.32	301	85.71	1.7788	Whitloctite
15	52.01	112	58.92	1.7569	β -calcium phosphate
16	59.40	311	64.38	1.5547	Hydroxyapatite
17	64.77	202	68.15	1.4382	Aragonite
18	64.91	122	60.01	1.4354	Apatite
19	66.52	040	54.78	1.4045	Hydroxyapatite
20	72.01	141	50.64	1.3104	Oxyapatite
21	77.41	413	46.15	1.2319	Hydroxyapatite

XRD spectra of the sample specimen are shown in the diffractogram in Figure 15. As it is seen from the diffractogram in Plate 4 that there are no crystalline peaks at the lower region in this graph which confirms the amorphous nature of the samples and exhibited a typical crystalline glass phase pattern with a glass hump. The SEM micrographs of the eggshell-derived hydroxyapatite particles are as shown in Figure 16.

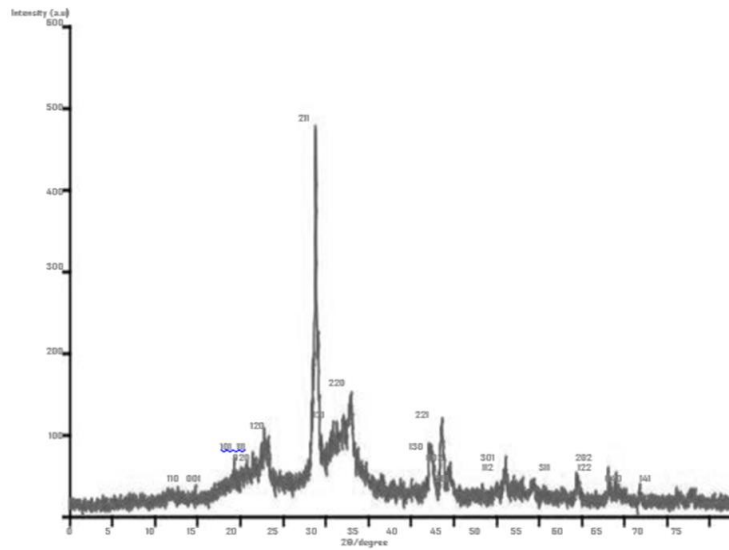


Figure 15: XRD diffraction pattern of eggshell derived HAp particles.

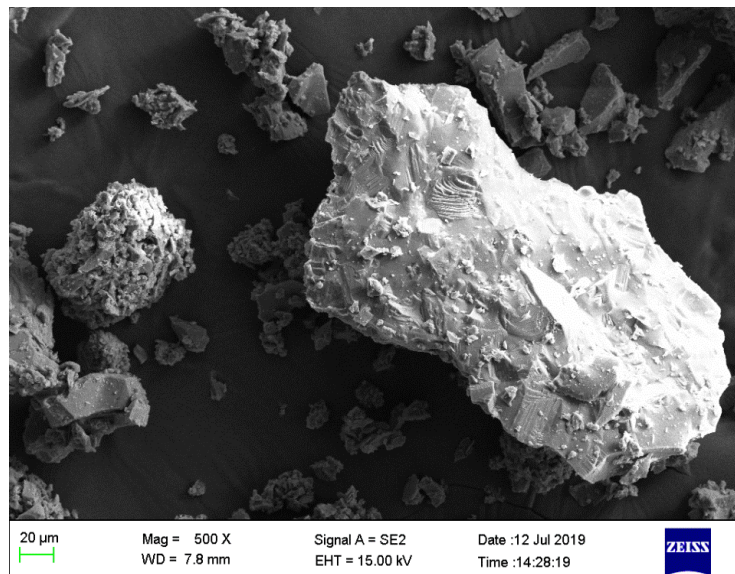


Figure 16: SEM Image of eggshell derived HAp particles.

3.9 SEM Images of The Developed Bio-Composites

Figure 17 shows the SEM image of the bio-composite sample with 3 wt.% eggshells derived HAp. It vividly revealed an even dispersion of the eggshell-derived HAp reinforcement particles in the epoxy matrix. It also indicated and confirmed a less amount of eggshell derived HAp particles when compared to other weight fractions and this led to a low agglomeration rate and the inclusion of pores in the 3 wt.% bio-composite sample. This low-weight fraction of eggshell-derived HAp dispersed in the epoxy matrix as observed in Plate 6 played a major role in the poor enhancements of the wear, hardness, impact, and thermal conductivity properties. The conspicuous uniform dispersion of the 3 wt.% weight fraction reinforcements triggered the optimum enhancement in the maximum tensile strength observed in Figure 4.

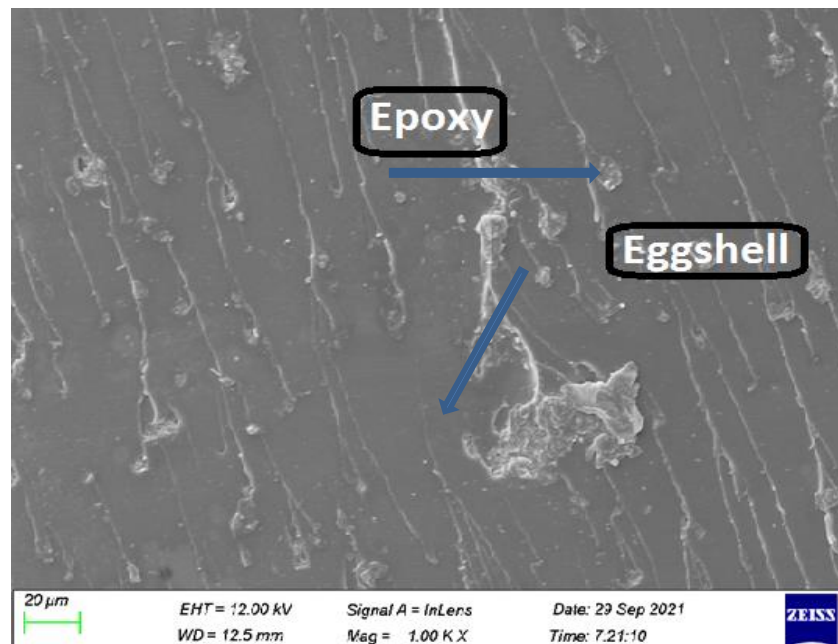


Figure 17: Bio-composite sample with 3 wt.% eggshells derived Hap.

The SEM image of the bio-composite sample with 6 wt.% eggshell derived HAp is shown in Figure 18. It was observed that a less visible even dispersion occurred in the matrix when compared to the 3 wt.% bio-composite sample and this occurred due to the increase in the weight fraction. A less conspicuous amount of agglomeration was indicated. This agglomeration detected was responsible for the poor enhancements in the maximum tensile and flexural strength properties as stated in Figure 4 and Figure 7, respectively.

Figure 19 showed the SEM image of the Bio-composite sample with 9 wt.% eggshells derived HAp. A more pronounced amount of eggshell particles was revealed with a more even dispersal. Also, a more conspicuous agglomeration was observed when compared to Figures 17 and 18. This more pronounced agglomeration observed in Figure 19 may be the reason for poor tensile and flexural properties as shown in Figure 4 to Figure 9. The presence of agglomeration also led to minimal enhancements in the hardness, impact and wear properties as observed in Figures 10, 11, and 14, respectively. There were enhancements in the thermal conductivity and water

absorption properties of the bio-composite sample with 9 wt.% reinforcement as observed in Figures 12 and 13, respectively. These enhancements in Figures 12 and 13 occurred due to the presence of an increase in the weight fraction when compared to Figures 17 and 18.

The SEM image of the bio-composite sample with 12 wt.% eggshell derived HAp is shown in Figures 20. This reveals an increase in the quantity of eggshell-derived HAp reinforcement particles with an even dispersal in the epoxy matrix. This increase in the quantity (weight fraction) of the eggshell-derived HAp particles observed in Figure 20 was responsible for the simultaneous increase in the hardness, impact, wear, thermal conductivity, and water absorption properties as shown in Figure 10 to Figure 14.

Figures 21 shows the SEM image of the Bio-composite sample with 15 wt.% eggshells derived HAp. A more visible amount of eggshell reinforcements was observed which led to the presence of agglomeration. The increase in the weight fraction observed in Figures 21 confirmed an increase in the density of the 15 wt.% composites. This increase in density was the sole factor responsible for the optimum enhancements in the mechanical, thermal conductivity, water absorption, and wear properties as shown from Figure 10 to Figure 14. Also, the tensile properties of the 15 wt.% reinforced composite were observed to be poor due to the presence enormous amount of the agglomeration shown in Plate 10.

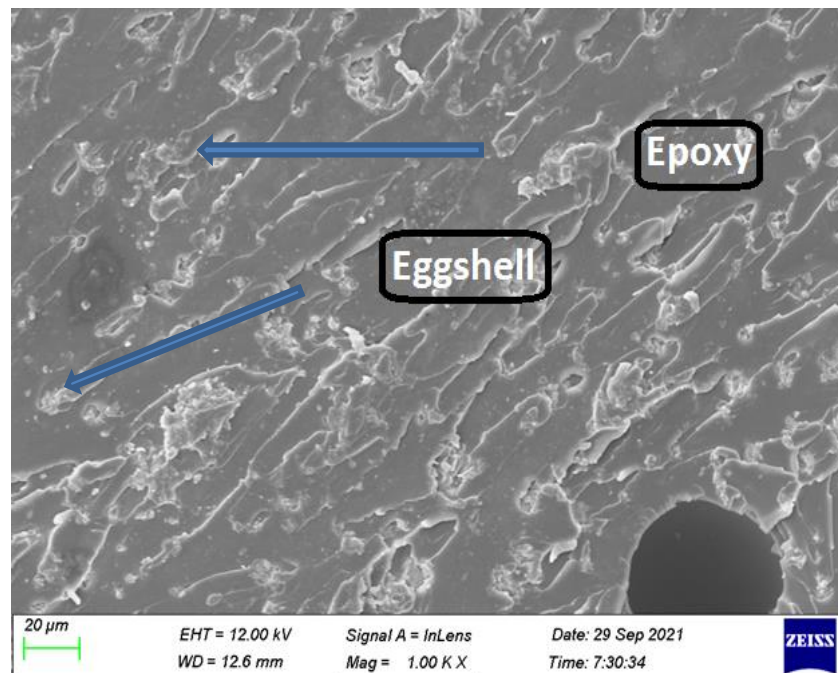


Figure 18: Bio-composite sample with 6 wt.% eggshells derived HAp.

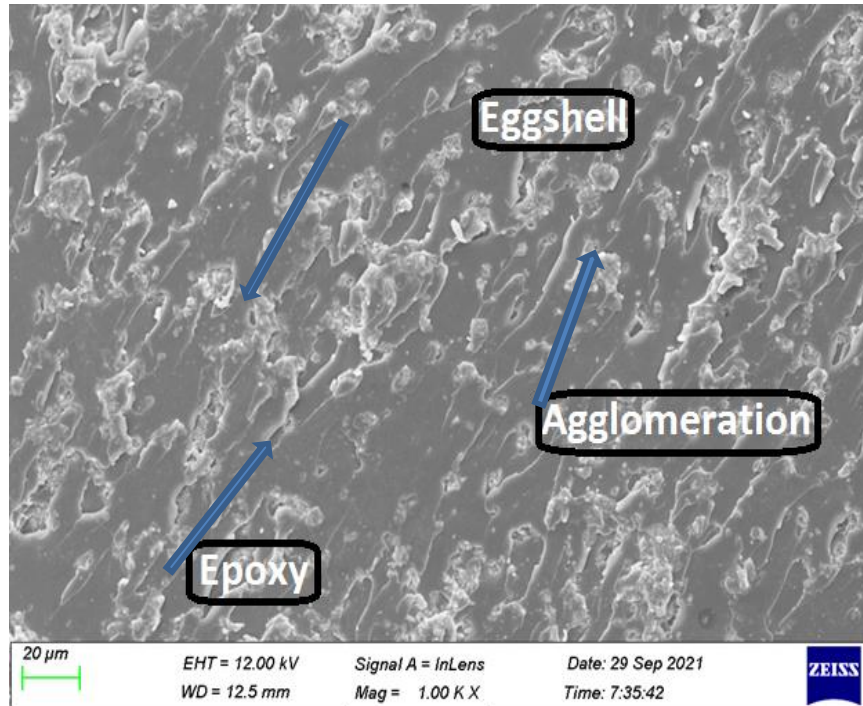
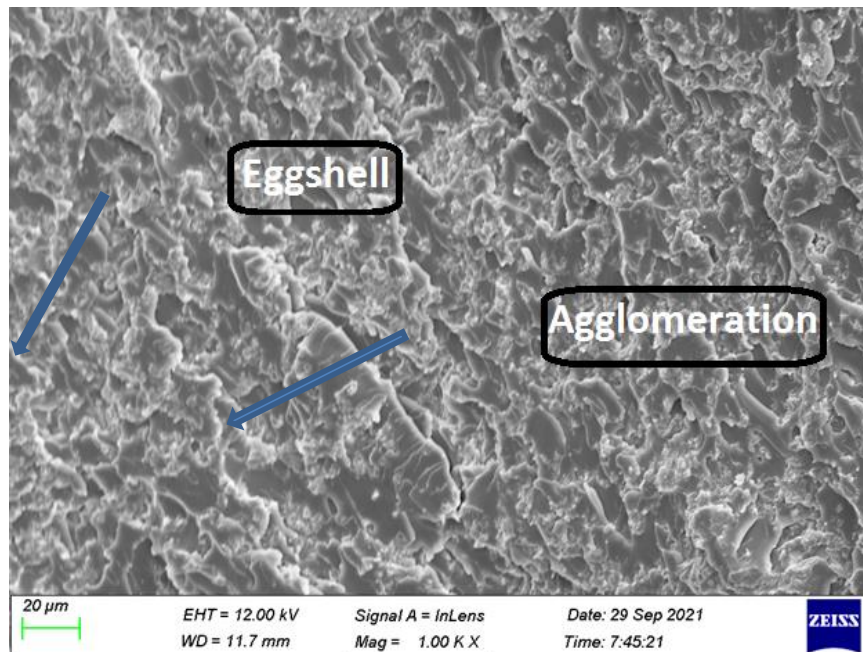
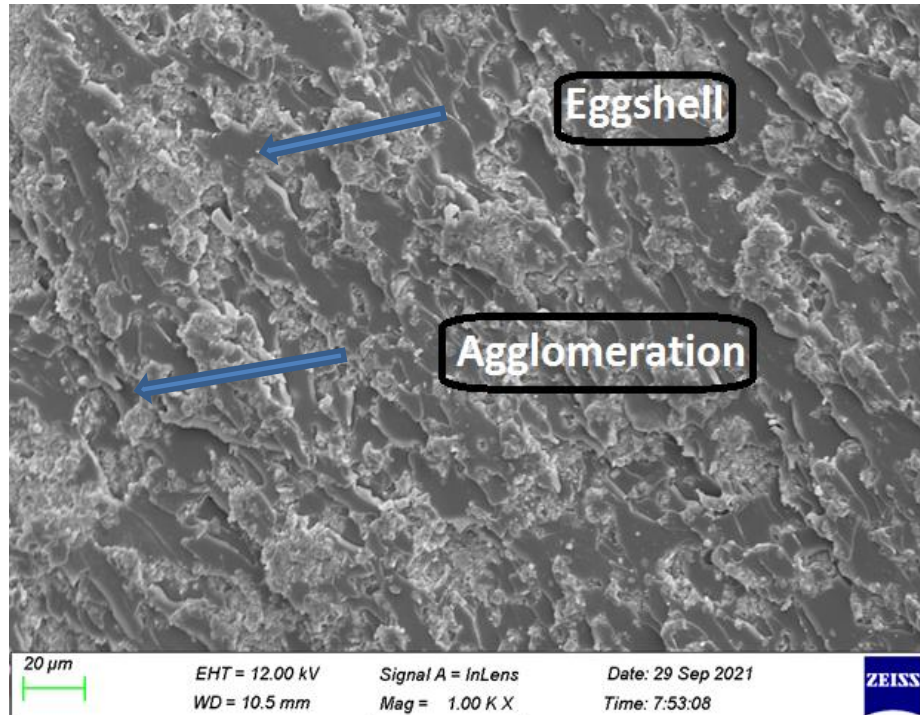


Figure 19: Bio-composite sample with 9 wt.% eggshell derived HAp.



Figures 20: Bio-composite sample with 12 wt.% eggshell derived HAp.



Figures 21: Bio-composite sample with 15 wt.% eggshells derived HAp.

CONCLUSIONS

Eggshell-based HAp was conscientiously synthesized from poultry eggshell waste and was reinforced in predetermined fractions into the epoxy matrix to form epoxy-based bio-composites. This research was carried out to investigate the feasibility of exploiting eggshell-derived HAp particles in the epoxy matrix as reinforcements for biomedical applications. From the research carried out, it was discovered that the addition of eggshell-derived HAp particles as reinforcements in epoxy resin aided better wear, thermal, water absorption, and mechanical properties. There were better and optimum enhancements in the wear, thermal, water absorption, hardness, and impact properties when compared to the tensile and flexural properties. Also, the 15 wt.% reinforced composite was observed and concluded to be the optimum weight fraction with the most improved properties when compared altogether. The developed composites showed improved properties compared to the control sample from the results, hence, they can be used as potential reinforcement materials for biomedical applications. Also, the synthesized eggshell-derived HAp particles are suitable for bone grafting applications.

ACKNOWLEDGMENTS

This work was supported through the AESA-RISE Fellowship Program [ARPDF 18-03], African Materials Science and Engineering Network (A Carnegie-IAS RISE network), and the DST-NRF Centre of Excellence in Strong Materials. AESA-RISE is an independent funding scheme of the African Academy of Sciences (AAS) implemented with the support of the Carnegie Corporation of

New York. At The AAS, AESA-RISE is implemented through AESA, the Academy's agenda and programmatic platform, created in collaboration with the African Union Development Agency (AUDA-NEPAD). The views expressed in this publication are those of the author(s) and not necessarily those of the AAS, AUDA-NEPAD, or Carnegie Corporation. The services of Dr. M. O. Bodunrin of the Department of Chemical and Metallurgical Engineering, University of the Witwatersrand, South Africa, in carrying out SEM analysis are appreciated.

REFERENCES

- Agbabiaka O. G., Oladele I. O., Akinwekomi A. D., Adediran A. A., Balogun A. O., Olasunkanmi O. G., Olayanju T. M. A., (2020). Effect of Calcination Temperature on Hydroxyapatite Developed from Waste Poultry Eggshell. *Scientific African Journal*, 8, 1-12, <https://eprints.lmu.edu.ng/id/eprint/2808>.
- Agbeboh, N. I., Oladele, I. O., Daramola, O. O., Adediran, A. A., Olasukanmi, O. O., and Tanimola, M. O. (2020). Environmentally Sustainable Processes for The Synthesis of Hydroxyapatite. *Heliyon*, 6 (4), 1-13, <https://doi.org/10.1016/j.heliyon.2020.e03765>.
- Ahmed, A. M. H., Rodriguez-Navarro, A. B., Vidal, M. L., Gautron, J., García-Ruiz, J. M. and Nys, Y. (2005). Changes in Eggshell Mechanical Properties, Crystallographic Texture, and in Matrix Proteins Induced by Moulting in Hens. *British Poultry Science*, 46 (3), 268-279, <https://doi.org/10.1080/00071660500065425>.
- Alizadeh-Osgouei M., Li Y., and Wen C. (2018). A comprehensive Review of Biodegradable Synthetic Ceramic Composites and their Manufacture for Biomedical Application, *Bioactive Materials*, 4 (1) 22-36, <https://doi.org/10.1016/j.bioactmat.2018.11.003>.
- Araya A. B, Anthony N. S, Mark K, Yanxi L., and Daniel T. R (2019). Mechanical Properties of Sisal-Epoxy Composites as Functions of Fiber-To-epoxy Ratio AIMS. *Materials Science*, 6 (6) 985-996, <http://dx.doi.org/10.3934/mat.2019.6.985>.
- ASTM D256-10 (2018): Standard Test Methods for Determining the Izod Pendulum Impact Resistance of Plastics, ASTM International, West Conshohocken, PA.
- ASTM D4060-10 (2018): Standard Test Method for Abrasion Resistance of Organic Coatings by the Taber Abraser, ASTM International, West Conshohocken, PA.
- ASTM D5229M-12 (2012): Standard Test Method for Moisture Absorption Properties and Equilibrium Conditioning of Polymer Matrix Composite Materials, ASTM International, West Conshohocken, PA.
- ASTM D638-14, (2014): Standards Test Method for Tensile Properties of Plastics: ASTM International, West Conshohocken, PA.
- ASTM D790-15, (2015): Standard Test Methods for Flexural Properties of Unreinforced and Reinforced Plastics and Electrical Insulating Materials, ASTM International, West Conshohocken, PA.
- ASTM E1530-19 (2019): Standard Test Method for Evaluating the Resistance to Thermal Conductivity by the Guarded Heat Flow Meter Technique ASTM International, West Conshohocken, PA.
- Balan G. S., Kumar V. S., Rajaram S., and Ravichandran M., (2020), Investigation on water absorption and wear characteristics of waste plastics and seashell powder reinforced polymer composite, *Jurnal Tribologi*, 27, 57 – 70, E-ISSN: 2289 – 7232.

- Bello, S.A., Agunsoye, J.O., Hassan, S.B., Zebase, S.G., Raheem I.A., (2015) Epoxy-Resin Based Composites, Mechanical and Tribological Properties: A Review, *Tribology in Industry*. 37(4), 500-524.
- Bhaskar J. and Singh V. K. (2013). Physical and Mechanical Properties of Coconut Shell Particle Reinforced-Epoxy Composite, *Journal of Materials and Environmental Science*, 4 (2), 227-232, ISSN: 2028-2508.
- Composite for Biomedical Application. *Journal of Applied Biotechnology and Bioengineering*, 1(1), 35 – 40, DOI: 10.15406/jabb.2016.01.00006.
- Daramola O. O, Olajide J. L, Oladele I. O., Adediran A. A, Adewuyi B. O., Muhammed A. A., and Sadiku E. R (2020) Mechanical and wear behaviour of polylactic acid matrix composites reinforced with crab-shell synthesized chitosan microparticles, *Materials Today: Proceedings*, 38 (2), 999–1005, <https://doi.org/10.1016/j.matpr.2020.05.599>.
- Ducheyne P., Raemdonck W., Heughebaert J.C, and Heughebaert M. (1986). Structural Analysis of Hydroxyapatite Coatings on Titanium, *Biomaterials*, 7 (2) 97–103, <https://doi.org/10.1016/0142-9612%2886%2990063-3>.
- Elizondo-Villarreal N., Martinez-De-La-Cruz A., Guerra R. O., Gomez-Ortega J. L., Torres-Martinez high-density polyethylene bio-composites. *Heliyon*, 5(10) 25-52, <https://doi.org/10.1016/j.heliyon.2019.e02552>.
- Kolawole S. A, Zakariyaw A. A, and Omoniyi A. O (2019). Preparation and Characterization of Epoxy Filled Snail Shell Thermoset Composite, *Direct Research Journal of Chemistry and Material Science* 6 (2), 8–13, DOI: <https://doi.org/10.5281/zenodo.3360904>.
- L. M., and Castano V. M. (2012). Biomaterials from Agricultural waste: Eggshell-based Hydroxyapatite. *Water, Air, and Soil Pollution*, 223 (7), 3643–3646, <https://doi.org/10.1007/s11270-012-1137-1>.
- Mulijani S., and Sulistyso G. (2012). Formation and Characterization of Hydroxyapatite/Chitosan Composite: Effect of Composite Hydroxyapatite Coating and its Application on Biomedical Materials, *Chemistry of Phytopotentials: Health, Energy and Environmental Perspectives*, 177 – 182, Springer, Berlin, Heidelberg. https://doi.org/10.1007/978-3-642-23394-4_38.
- Nys, Y., Gautron, J. Garcia-ruiz, J. M. and Hincke M. T., (2004). Avian eggshell mineralization: biochemical and functional characterization of matrix proteins, *Comptes Rendus Palevol*, (3), 549 – 562, <https://doi.org/10.1016/j.crpv.2004.08.002>.
- Oladele I. O, Agbabiaka O. G., Olasunkanmi O. G., Balogun A. O., and Popoola M. O. (2018a) non-synthetic sources for the development of hydroxyapatite. *Journal of Applied Biotechnology and Bioengineering*, 5(2), 92–99, DOI: 10.15406/jabb.2018.05.00122.
- Oladele I. O., and Isola B. A. (2016) Development of bone particulate reinforced epoxy composite for biomedical application. *J Appl Biotechnol Bioeng*. 1(1):35-40. DOI: 10.15406/jabb.2016.01.00006.
- Oladele I. O., Makinde-Isola B. A., Agbeboh N. I., and Iwarere B. O., (2020b) Thermal Stability, Moisture Uptake Potentials and Mechanical Properties of Modified Plant-Based Cellulosic Fiber-Animal Wastes Hybrid Reinforced Epoxy Composites, *Journal of Natural Fibers*, 17(12), 1-16, DOI: 10.1080/15440478.2020.1863290.
- Oladele I. O., Omotosho T. F. Ogunwande G. S. and Owa F. A. (2021) A Review on the Philosophies for the Advancement of Polymer-based Composites: Past, Present and Future Perspective, *Applied Science and Engineering Progress*, 14(4) (Special Issue), 553–579, <http://dx.doi.org/10.14416/j.asep.2021.08.003>.

- Oladele I. O., Omotosho T. F., and Adediran A. A. (2020a) Polymer-Based Composites: An Indispensable Material for Present and Future Applications, *International Journal of Polymer Science (Hindawi)*, 1 (20): 1-12.
- Oladele, I. O., Agbabiaka, O. G., Adediran A. A., Akinwekomi A. D., and Balogun A. O. (2019), Structural performance of poultry eggshell derived hydroxyapatite based high density polyethylene bio-composites, *Heliyon*, Volume 5, Issue 10, e02552, <https://doi.org/10.1016/j.heliyon.2019.e02552>.
- Oladele, I. O., Akinola, O. S., Agbabiaka, O. G., and Omotoyinbo, J. A. (2018b). Mathematical Model for the Prediction of Impact Energy of Organic Material Based Hydroxyapatite (HAp) Reinforced Epoxy Composites. *Fibers and Polymers*, 19(2), 452- 461
- Oliveira I. R., Andrade T. L., Araujo K. C. M. L., Luz A. P., and Pandolfelli V. C. (2016). Hydroxyapatite Synthesis and the Benefits of its Blend with Calcium Aluminate Cement. *Ceramics International*, 42(2), 2542-2549, DOI: <http://dx.doi.org/10.1016/j.ceramint.2015.10.056>.
- Owuamanam S. I (2019), Fabrication and Characterization of Bio-epoxy Eggshell Composites: A Master's Dissertation Submitted to the College of Graduate and Postdoctoral Studies, Department of Mechanical Engineering, University of Saskatchewan Saskatoon.
- Patricio, T., Raul. Q., Yazdani-Pedram M., and Arias J. L., (2007). Eggshell, A New Bio-Filler for Polypropylene Composites, *Materials Letters*, 61 (22), 4347-4350, <http://repositorio.uchile.cl/handle/2250/120809>.
- Ramesh M., Sri A. T., Aswin U. S., Eashwar H., and Deepa C. (2014). Processing and Mechanical Property Evaluation of Banana Fiber Reinforced Polymer Composites. *Procedia Engineering*, 97, 563-72, <https://doi.org/10.1016/j.proeng.2014.12.284>.
- Shuhadah, S., Supri M., Kamaruddin, H., (2008). Thermal Analysis, Water Absorption and Morphology Properties of Eggshell Powder Filled Low-Density Polyethylene Composites, *Proceeding of MUCET 2008, UniMAP, Kangar, Perlis*, 15 - 16 March 2008.
- Teboho C. M., Mokgaotsa J. M., Tshwafo E. M., Linda Z. L., Oriel M. T, and Sandile P. S. (2018) Sugarcane bagasse and cellulose polymer composites. *Technology and Research*, 12: 225-241, DOI: 10.5772/intechopen.71497.
- Thomas A., Lee P. J., and Dalton J. E., (2012). Polymer-Based Biomaterials. *Technology and Research*, (5) 456 - 447.